

## Tumorigenesis and Neoplastic Progression

# Angiopoietin-1 Promotes Tumor Angiogenesis in a Rat Glioma Model

Marcia Regina Machein,\* Anette Knedla,<sup>†</sup>  
Rolf Knoth,<sup>‡</sup> Shawn Wagner,<sup>§</sup> Elvira Neuschl,\* and  
Karl H. Plate<sup>†</sup>

From the Department of Neurosurgery,\* University of Freiburg Medical School, Freiburg, Germany; the Institute of Neurology (Edinger Institute),<sup>†</sup> University of Frankfurt Medical School, Frankfurt, Germany; the Department of Neuropathology,<sup>‡</sup> University of Freiburg Medical School, Freiburg, Germany; the Department of Experimental Cardiology,<sup>§</sup> Max-Planck-Institute for Physiological and Clinical Research, Bad Nauheim, Germany

**Angiopoietins have been implicated in playing an important role in blood vessel formation, remodeling, maturation, and maintenance. However, the role of angiopoietins in tumor angiogenesis remains uncertain. In this study, expression of human angiopoietin-1 (hAng-1) and angiopoietin (hAng-2) was amplified in the rat glioma cell line GS9L by stable transfection using an inducible tet-off system. Transfected cells were implanted intracerebrally into syngenic Fischer 344 rats. We demonstrated by means of magnetic resonance imaging that increased hAng-1 expression promoted a significant *in vivo* growth of intracerebral gliomas in rats. Overexpression of hAng-1 resulted in more numerous, more highly branched vessels, which were covered by pericytes. On the other hand, tumors derived from hAng-2-overexpressing cells were smaller than empty-plasmid control tumors. The tumor vasculature in these tumors was composed of aberrant small vascular cords, which were associated with few mural cells. Our results indicate that in the presence of hAng-1, tumors induce a more functional vascular network, which led to better tumor perfusion and growth. On the other hand, overexpression of hAng-2 led to less intact tumor vessels, inhibited capillary sprouting, and impaired tumor growth. (*Am J Pathol* 2004, 165:1557–1570)**

Angiogenesis is a complex multi-step process by which new vessels are formed from pre-existing blood vessels. This process requires complex signaling pathways and a

high degree of spatial and temporal orchestration of various cell types and multiple pro- and anti-angiogenic factors and their corresponding receptors.<sup>1</sup> Until recently, most work in the field was focused on growth factors with mitogenic properties to endothelial cells like fibroblast growth factor and vascular endothelial growth factor (VEGF).<sup>2</sup>

Recently, growing interest has been directed upon a novel family of endothelial growth factors, the angiopoietins. Angiopoietin-1 (Ang-1) and its antagonist angiopoietin-2 (Ang-2) each signal via the Tie-2 receptor tyrosine kinase expressed on endothelial cells.<sup>3,4</sup> Unlike other endothelial cell growth factors, neither Ang-1 nor Ang-2 produce a mitogenic response on cultured endothelial cells.<sup>3</sup> Ang-2 appears to block the activation of Tie-2 by Ang-1, suggesting that it may be a naturally occurring inhibitor of Ang-1.<sup>4</sup> Similar to VEGF, Ang-1 is essential for normal vascular morphogenesis, since disrupting the function of either the Ang-1 or Tie-2 genes result in embryonic lethality in mice.<sup>5</sup> Consistent with its proposed role as an Ang-1 antagonist, transgenic overexpression of Ang-2 in endothelial cells results in lethal embryonic defects comparable to those observed in Ang-1 and Tie-2-deficient mice.<sup>4</sup> Increasing evidence suggests that the Tie-2/angiopoietin system is involved in the interaction between endothelial cells and supporting periendothelial cells. Ang-1 has been proposed to stabilize the adult vasculature by promoting the recruitment of supporting periendothelial cells.<sup>5–7</sup> Ang-2 has been thought to block the stabilization effects of Ang-1, thereby facilitating the angiogenic response in presence of VEGF, or inducing vessel regression in the absence of VEGF.<sup>4</sup>

Conflicting results have been reported in the literature regarding the role of the angiopoietin/Tie-2 system in

---

Supported by Mildred Scheel Stiftung für Krebsforschung grants 10–1596-Ma I and ZKF III (Schwerpunkt Angiogenese, Universitätsklinik Freiburg) (to M.R.M.) and BMBF 01 KV 0102 and DFG Pl158/6–1 (to K.H.P.).

M.R.M. and A.K. contributed equally to this work.

Accepted for publication July 8, 2004.

Address reprint requests to Karl H. Plate, Institute of Neurology (Edinger Institute), University of Frankfurt Medical School, Deutschordensstrasse 46, 60528 Frankfurt am Main, Frankfurt, Germany. E-mail: Karl.heinz.plate@kgu.de.

tumor angiogenesis. Whereas some recently published reports imply that overexpression of Ang-1 in different cancer cells has a pro-angiogenic effect,<sup>8</sup> other authors suggest that induction of Ang-1 impaired angiogenesis and therefore inhibited tumor growth.<sup>9–11</sup> The same contradictory results are also reported regarding overexpression of Ang-2 in different tumors, suggesting a pro- or anti-angiogenic effect of Ang-2 in tumors.<sup>12–15</sup>

One of the major pathophysiological characteristics of malignant gliomas is the ability to induce a robust angiogenic response.<sup>16</sup> Indeed, glioblastomas belong to the most vascularized tumors in humans. Previous work has shown that angiopoietins are expressed in gliomas and that their expression correlates with the malignancy grade.<sup>17–19</sup> However, the role of these proteins in glioma angiogenesis is not well known. We investigated the role of angiopoietins in glioma angiogenesis by overexpressing hAng-1 and hAng-2 in rat glioma cells and analyzing the tumor angiogenesis, tumor growth, and vascular permeability.

## Materials and Methods

### Cells and Cell Culture

Rat glioblastoma cell line GS9L was a gift from Tom Budd, St. Lawrence University, Canton, NY. Cells were cultured in RPMI medium with 10% fetal calf serum at 37°C in 5% CO<sub>2</sub>, 95% air.

### Vector Construction and Stable Transfection of GS9L Cells

A vector containing bi-directional expression cassettes, in which seven centrally located copies of the tet-operator sequence are flanked by minimal promoters from the human CMV immediate early gene that direct expression of hAng-1 or hAng-2 on one side and a fusion of enhanced green fluorescent protein (EGFP) with neomycin phosphotransferase on the other side was constructed. Both constructs were verified for appropriate orientation and absence of mutations by sequence analysis. GS9L cells were co-transfected with either the hAng-1 or the hAng-2 construct and the cytomegalus virus (CMV) promoter/enhancer-driven tTA plasmid pUHDxxx (a gift from H. Bujard, Heidelberg, Germany) using superfect reagent (Qiagen, Hilden, Germany) according to the manufacturer's protocol. Clones expressing the fusion of EGFP/neomycin-phosphotransferase were selected in the presence of the neomycin-analog G418. Isolated EGFP-positive clones were tested for expression of hAng-1 or Ang-2 by Western and Northern blotting.

### Western Blotting

GS9L cells and stable transfectants were grown to sub-confluency, washed twice with ice-cold phosphate-buffered saline (PBS), and harvested by scraping. Ultrasonic homogenization of cells was done in 150  $\mu$ l homogeni-

zation buffer (50 mmol/L Tris, 150 mmol/L NaCl, 0.02% NaN<sub>3</sub>, 0.1% SDS, 1% NP-40, 0.5% sodium deoxycholate, 1  $\mu$ g/ml aprotinin, and 100  $\mu$ g/ml PMSF). Serum-free supernatants from parental GS9L and stable-transfected clones were collected and concentrated using Chemicon Plus 20 filters (Millipore, Bradford, MA).

Total concentration of protein in supernatants and cell fraction was determined by the method of Bradford. An equal amount of protein from each sample was loaded to a 10% SDS-PAGE. Proteins were electroblotted onto a nitrocellulose membrane and blocked with 5% nonfat milk/PBS with 0.1% Tween 20 for 1 hour at room temperature. The membrane was incubated with the first antibody (purified goat anti-human Ang-1 or purified goat anti-human Ang-2; dilution for both antibodies 1:100; Santa Cruz Biotechnology Inc., Santa Cruz, CA). After washing the membrane three times in 5% nonfat dry milk/PBS with 0.1% Tween 20, the membrane was incubated with peroxidase-conjugated donkey anti-goat IgG (dilution 1:2000; Dianova, Hamburg, Germany) for 1 hour, following a triple-wash step and development of the blot. As loading control, the membrane was probed with monoclonal anti- $\beta$ -tubulin (dilution 1:5000; Sigma-Aldrich, St. Louis, MO) as first antibody and donkey anti-mouse IgG (dilution 1:10,000; Dianova) as second antibody.

### ELISA

Cells were cultured in RPMI medium with 10% fetal calf serum at 37°C in 5% CO<sub>2</sub>, 95% air. Hypoxia conditions were 1% O<sub>2</sub> at 37°C for 18 hours. Serum-free supernatants from parental GS9L and stable-transfected clones were collected and concentrated using Chemicon Plus 20 filters (Millipore). ELISA test for hAng-2 was purchased from R&D Systems (Minneapolis, MN). It was performed according to the manufacturer's protocol. Concentrated cell culture supernatants were diluted 1:100 or 1:500, respectively. Color development was measured at 450 nm using a microplate reader (SLT-Genios, SLT-Instruments, Crailsheim, Germany). Concentrations were calculated using SLT-software.

### Northern Blot Analysis

GS9L wild-type and transfected cells ( $2 \times 10^6$ ) were plated into 100-mm culture dishes. Total RNA was extracted with the Qiagen RNA Isolation Kit (Rneasy Total Kit, Qiagen) according the manufacturer's instructions. Ten  $\mu$ g of RNA were electrophoresed in a 1.5% agarose gel containing 15% formaldehyde and subsequently transferred to a Duralon membrane (Stratagene, La Jolla, California) in 10X SSC. Filters were cross-linked with UV light (0.4J/cm<sup>2</sup>) and hybridized at 68°C in hybridization solution (QuickHyb, Stratagene) with the following random-primed <sup>32</sup>P- labeled cDNA probes: a full-length cDNA encoding for the hAng-1 and a full-length cDNA encoding for the hAng-2. For RNA loading, we used a cDNA-fragment encoding for chicken  $\beta$ -actin. Densitom-

etry was performed using TINA 2.0 Software, Version 2 (Raytest, GmbH/Straubenhardt).

### *Intracerebral Glioma Model*

All procedures with animals were performed according to the institutional guidelines for use of laboratory animals. Syngenic male rats (Fischer 344), weighing between 250 to 300 g, were purchased from Charles River (Sussfeld, Germany). Cells were trypsinized, washed twice, and resuspended in PBS.  $10^5$  cells were stereotactically inoculated in a final volume of 10  $\mu$ l in the right caudatum as described previously.<sup>20</sup> Twelve animals were inoculated per group. Animals were sacrificed 9 days after tumor implantation.

### *Magnetic Resonance Imaging (MRI) and Evaluation of Tumor Volume*

On the ninth day after tumor implantation, animals were anesthetized from the four groups (wild-type, vector only, hAng-1, and hAng-2) with 1.6% isoflurane (Abbott GmbH & Co. KG, 65205 Wiesbaden, Germany) in a 20/80 oxygen/air gas stream. A Bruker PharmaScan 7.0 Tesla magnetic resonance imager was used to acquire T2 weighted images using a 2-D spin-echo sequence, TR (repetition time)/TE (echo time) = 1000/20, with an in-plane resolution of 100  $\mu$ m and a slice thickness of 0.62 mm. Scout scans were done to determine the location of the brain. The rat was then scanned and removed from the magnetic and subsequently received a dose of 0.75 mmol/kg of gadolinium DPTA (Magnevist, Schering Deutschland GmbH, 10589 Berlin, Germany) and placed back in the magnetic in the same position. Serial scans were obtained after contrast medium injection every minute for up to 10 minutes after injection.

Tumor sizes were calculated 10 minutes after contrast injection. The tumor volume was calculated by manually tracing the boundary of the contrast-enhanced tumor within each cross-section (defined as region of interest, ROI). The area of the each ROI was multiplied by the slice thickness. This procedure was repeated for all slices showing contrast-enhanced tumor and the areas were summed to determine total tumor volume.

### *Measurement of Vascular Permeability in Brain Tumors Using Evans Blue*

Immediately after MRI, permeability to Evans blue was evaluated according to the method described previously.<sup>21</sup> In brief, Evans blue dye (2% saline, 3 ml/kg) was administered intravenously and allowed to circulate for 60 minutes. To remove intravascular dye, animals were perfused with saline through the left ventricle until colorless fluid was obtained from the right atrium. Brains were removed, sectioned, weighed, and frozen in liquid nitrogen. The ipsilateral and contralateral hemispheres were homogenized in 2 ml of 50% trichloroacetic acid (w/v) and centrifuged at 10,000 rpm for 20 minutes. After cen-

trifugation, the supernatants were collected and diluted twofold in 50% trichloroacetic/acid. Tissue levels of Evans blue were quantified using a spectrofluorometer at an excitation wavelength of 620 nm and an emission wavelength of 680 nm. Sample values were compared with those of standards. Results were expressed in nanogram per milligram of tissue.

### *In Situ Hybridization*

For *in situ* hybridization 10- $\mu$ m frozen sections were mounted on positively charged superfrost slides (Fisher Scientific Co., Houston, TX) and dried at 50°C. Afterward, sections were fixed for 15 minutes in 4% paraformaldehyde and dehydrated in a series of ethanol (30%, 60%, 80%, 95%, and 100%, 5 minutes each). Slides were air-dried and stored at -80°C before use.

RNA probes were generated as described previously.<sup>17</sup> Briefly, plasmids were linearized and single-stranded transcripts were synthesized from the T<sub>7</sub>/T<sub>3</sub> polymerase promoters using digoxigenin (DIG)-labeled UTP as substrate. We used the following as probes: a mouse VEGF<sub>164</sub> cDNA subcloned in pBluescript KS<sup>+</sup>, a mouse Ang-1 cDNA subcloned in pBluescript KS<sup>+</sup>, a mouse Ang-2 cDNA subcloned in pBluescript KS<sup>+</sup>, and a mouse Tie-2 cDNA subcloned in pGEM-T.

### *Free-Floating Immunofluorescence and Confocal Analysis*

Two animals per group were perfused with PFA 4% in PBS. Brains were post-fixed in PFA 4% for 24 hours. Coronal brain sections (60  $\mu$ m) were cut on a Vibratome (Leica). Free-floating sections were incubated with a rabbit anti-vWF (1:200, Dako, Denmark). Sections were then incubated with Cy3-labeled goat anti-rabbit (1:500, Jackson ImmunoResearch, West Grove, PA). After washing, sections were mounted and analyzed with krypton-argon laser scanning confocal imaging system (Leica, Heidelberg, Germany). EGFP was imaged with excitation at 495 nm and emission at 510 nm. Cy3 was imaged with excitation at 547 nm and emission above 572 nm. Microscopic data were acquired with  $\times 20$  and  $\times 40$  oil-immersion objective lens. Three-dimensional analysis was performed using Autovisualize Software (Autoquant Imaging, Inc).

### *TUNEL Reaction*

For detection of apoptotic cells, TUNEL assay (Tdt-mediated dUTP nick end labeling) was performed using the In Situ Cell Death Detection Kit AP (Alkaline Phosphatase) (Roche Diagnostics, Switzerland). Frozen 14- $\mu$ m sections were fixed and stained according to the manufacturer's instructions.

### *Indirect Immunofluorescence*

Brains were excised from experimental rats ( $n = 4$ /group) 9 days after tumor implantation, placed in Tissue-Tek

freezing medium and snap-frozen in liquid nitrogen. Cryosections (14  $\mu\text{m}$ ) were fixed in cold acetone and allowed to air dry. Slides were incubated with 1% bovine serum albumin (BSA) in PBS and stained with the following antibodies: rabbit anti-vWF (1:200, Dako) and mouse anti-smooth muscle-actin antibody (1:100, anti-SMA, Sigma, clone 1A4). The secondary antibodies, labeled with either Texas red or fluorescein isothiocyanate (Jackson ImmunoResearch) were used at a dilution of 1:500 and 1:200, respectively. Slices were washed, mounted, and photographed in a Leica confocal microscopy using a  $\times 20$  objective. Negative controls were performed using unspecific immunoglobulins (mouse IgG2a, BD Pharmingen, rabbit IgG, Dianova). Two independent observers analyzed randomized fields per section (three sections/animal) obtained from each animal (a total of four animals per group). The percentage of blood vessels associated with SMA-positive cells was defined as vessel maturation index according to the method described previously.<sup>22</sup>

### *Computer-Assisted Morphometric Analysis of Tumor Vessels*

Immunohistochemistry for endothelial cell marker CD31 was performed by indirect immunoperoxidase staining. Cryosections were fixed as described above and blocked for non-specific antibody binding with 2% normal goat serum, followed by incubation with a monoclonal mouse anti-rat CD31 (1:100, Serotec). Following three washes with PBS, sections were then incubated with biotinylated goat anti-mouse immunoglobulin containing 2% rat serum (Vector Laboratories, Burlingame, CA). After three PBS washes, sections were incubated with avidin-biotin complex reagent (Vector Laboratories) followed by 3,3'-diaminobenzidine (Vector Laboratories) according to the manufacturer's instructions. Slides were counterstained with hematoxylin. Photomicrographs were taken with Zeiss Axioplan 2 Imaging and Axion Vision 3 Software.

### *Assessment of Tumor Vessel Count and Capillary Density*

For assessment of the tumor vessel count, different fields in each section (three sections/animal with a total of four animals per group) were examined at a  $\times 10$  magnification. Blood vessels were counted using Soft Imaging Analysis System and classified according to vessel area (0 to 500  $\mu\text{m}^2$ , 500 to 2000  $\mu\text{m}^2$ , and  $>2000 \mu\text{m}^2$ ). To evaluate the capillary density, random pictures of tumors were examined at  $\times 20$  magnification. Capillary density is defined as percentage of vessel area with tumor area.

### *Electron Microscopy*

For electron microscopy analysis, rats ( $n = 2$ ) were perfused with 4% PFA. Thereafter, small tumor pieces (collected at the tumor border and tumor middle) were fixed

with 2.5% glutaraldehyde in Sorensen buffer post-fixed with  $\text{OsO}_4$ , and stained with uranyl acetate and lead citrate. Samples were examined in a Philips CM 100 electron microscope and in a Zeiss electron microscope 10c/CR.

### *Statistical Analysis*

The two unpaired *t*-test (SPSS, Inc, Chicago, IL) was used to analyze differences in tumor volumes, vessel count, vessel density, and vessel maturation index. A *P* value of less than 0.05 was considered statistically significant.

## *Results*

### *Expression of Biological Active Ang-1 and Ang-2 in Rat GS9L Glioma Cells*

We used a bidirectional vector, which allowed the expression of hAng-1 or hAng-2 simultaneously with the expression of EGFP and a neomycin-resistant cassette under the control of a tetracycline responsive element. Cell clones were selected with the neomycin-analog G418. EGFP expression was validated by fluorescence microscopy and fluorescent-activated cell sorter (FACS) (data not shown). EGFP-expressing clones were selected on expression of Ang-1 or Ang-2 on protein levels as determined by Western blot analysis (Figure 1A). A 5.6-fold up-regulation of Ang-1 and 8.9-fold up-regulation of Ang-2 could be detected in cell extracts from transfected clones compared to parental cells. Quantitative evaluation of Ang-2 in supernatant of transfected clones was performed using a commercially available ELISA test. A 19-fold increase in levels of secreted Ang-2 was observed in supernatants obtained from transfected cells. We cannot exclude that the level of Ang-2 was even higher since the amount of Ang-2 detected was in the upper detection limit of the test. This might explain why we could not detect a further increase in conditioned medium from GS9L-hAng-2 cells under hypoxic conditions.

As determined by Northern blot analysis, parental cells and vector only-transfected control clones expressed very low amounts of Ang-1 or Ang-2 mRNA, whereas the selected clone strongly expressed Ang-1 and Ang-2 transcripts (densitometry revealed a 37.9- and 29-fold up-regulation in levels of Ang-1 and Ang-2 mRNA, respectively; transfected clones in comparison with parental cells) (data not shown).

To confirm that overexpression of hAng-1 or hAng-2 in the experimental glioma cell line had no effect on tumor cell proliferation, we analyzed the growth curve of the transfected clones and parental cell line *in vitro*. No significant difference in growth rates was observed between the different transfected GS9L clones and the parental cell line (data not shown).

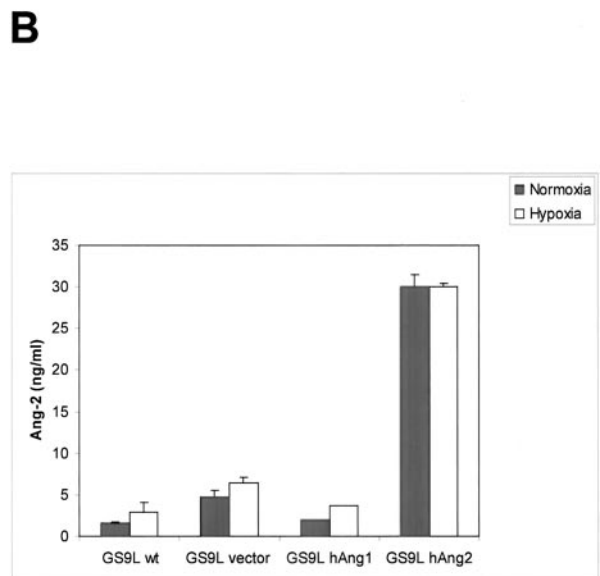
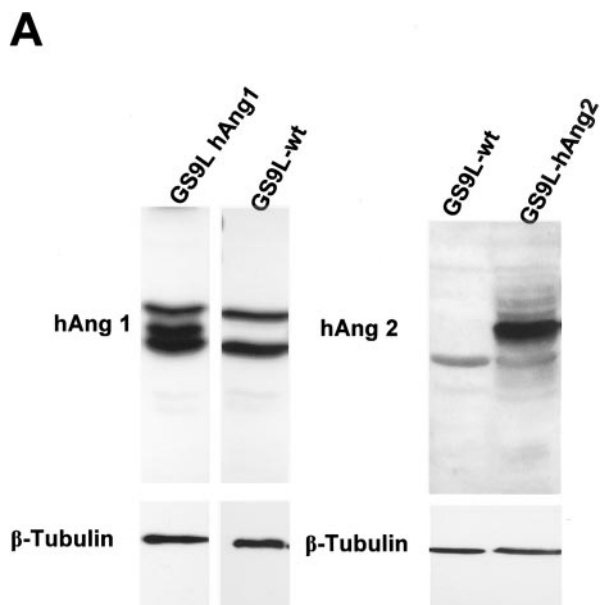


**Figure 1.** Overexpression of hAng-1 and hAng-2 in GS9L cells. **A:** Equal amounts of total protein obtained from cell fractions were loaded and analyzed by SDS-PAGE followed by Western blotting and detection of angiopoietins with a goat anti-human Ang-1 or a goat anti-human Ang-2 antibody. The membranes were subsequently stripped and incubated with an anti-tubulin antibody for loading control. No expression of angiopoietins was detected in GS9L parental cells. In selected clones Western blot confirmed the overexpression of hAng-1 and hAng-2 protein. **B:** GS9L and stable-transfected cells were cultivated under normoxic and hypoxic conditions. hAng-2 protein levels in serum-free conditioned media were evaluated using ELISA. A 19-fold increase in levels of secreted hAng-2 was observed in supernatants obtained from transfected cells. Hypoxia increases hAng-2 protein levels in conditioned media. In GS9L-hAng-2 cells expression levels at normoxia was already at detection limit of the test and further increase under hypoxia could not be detected.

### In Vivo GS9L Glioma Growth Is Enhanced by Ang-1

To evaluate the effects of hAng-1 or hAng-2 overexpression on the growth of experimental rat gliomas, transfected clones (hAng-1, hAng-2, and vector only) or the wild-type GS9L were intracerebrally implanted in syngenic Fischer rats. The experiments were terminated af-

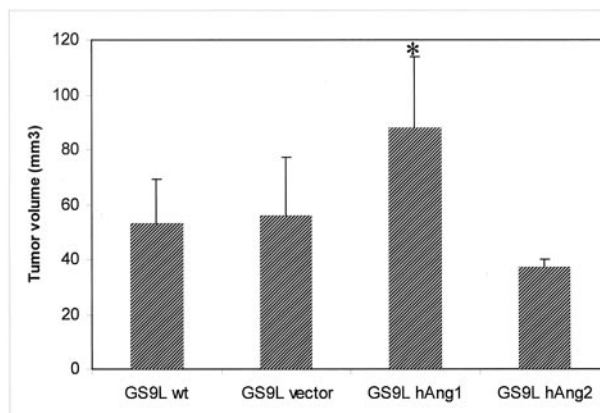


**Figure 2.** Intracranial glioma growth in syngenic rats. Wild-type and transfected cells ( $10^5$  in  $10 \mu\text{l}$  PBS) were injected intracerebrally in syngenic Fischer rats. Nine days after tumor implantation, rats were anesthetized and brains were scanned in a Bruker 7.0 Tesla without and with contrast injection. Tumor volume was calculated by determining the area of contrast-enhanced region in each image. The area in each section was multiplied by the slice thickness. Final volume represents the sum of all enhanced areas in a given tumor. Each bar represents the mean and SD of tumors from rats injected with the corresponding GS9L wild-type ( $n = 6$ ), GS9L-vector ( $n = 6$ ), GS9L-hAng-1 ( $n = 8$ ), and GS9L-hAng-2 ( $n = 6$ ). (\*,  $P < 0.05$  relative to the wild-type control tumors).

ter 9 days of tumor growth, when the tumor size had achieved a considerable volume but the rats did not develop visible symptoms of intracranial tumor growth. Tumor volume was assessed using contrast-enhanced magnetic resonance imaging. Parental GS9L cells and vector-only transfected cells formed rapidly growing tumors reaching a volume of  $52.6 \text{ mm}^3$  (SD = 16.8) and  $55.7 \text{ mm}^3$  (SD = 21.1), respectively. Overexpression of hAng-1 resulted in a statistically significant increase of tumor growth by more than 50% (tumor volume =  $88.0 \text{ mm}^3$ , SD = 26.3) compared to control tumors ( $P = 0.014$ ) (Figure 2). In contrast, overexpression of hAng-2 led to inhibition of tumor growth by 40% (tumor volume =  $36.8 \text{ mm}^3$ , SD = 3.4), which compared to the control tumors was not statistically significant ( $P = 0.070$ ) (Figure 2).

### In Vivo Expression of Angiopoietins, Tie-2, and VEGF in Experimental Tumors

We next performed *in situ* hybridization to characterize the expression of the angiopoietins, VEGF, and Tie-2 mRNA in the tumors. Ang-1 mRNA is expressed in wild-type and vector-transfected tumors at this development stage at very low levels. We found that in hAng-1-overexpressing tumors only a subset of tumor cells (about 20%) expressed Ang-1 mRNA, suggesting a down-regulation of the transgene expression *in vivo*. However, taking into account that control tumors express very low levels of Ang-1 mRNA, this up-regulation is considerable. Ang-2 was found to be expressed by tumor vessels at the tumor borders (Figure 3). hAng-2-overexpressing tumors showed a robust up-regulation of Ang-2 mRNA expression (about 60% of tumor cells expressed Ang-2 mRNA) (Figure 3). Expression patterns of Ang-1 and Ang-2 in the overexpressing tumors correlate with the amount of EGFP found at protein levels in the respective tumors.

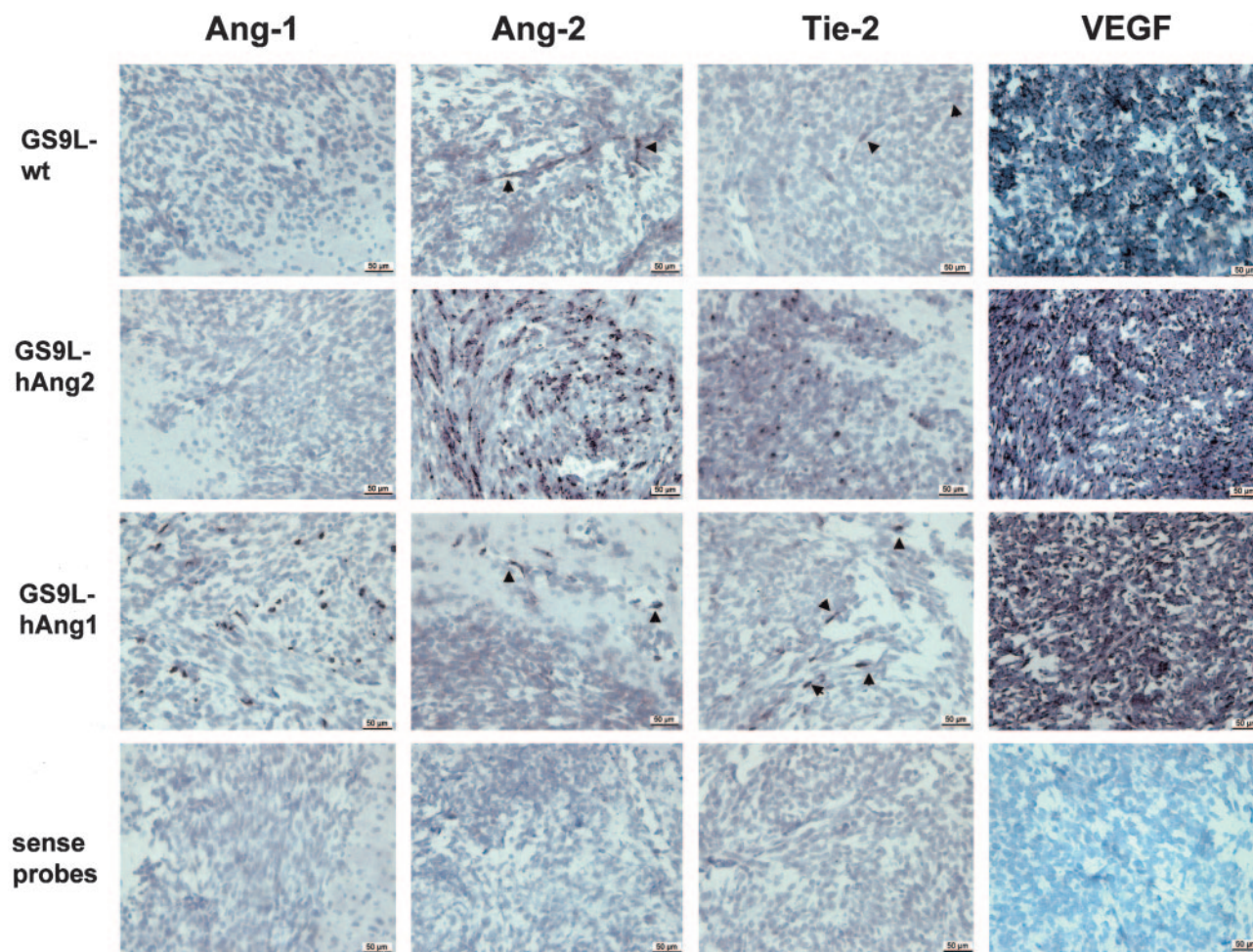


**Figure 3.** *In situ* hybridization analysis of Ang-1, Ang-2, Tie-2, and VEGF mRNA in wild-type, hAng-2-, and hAng-1-transfected tumors. At day 9 after tumor implantation, small amounts of Ang-1 mRNA are expressed in control and hAng-2-transfected tumors. Only a subset of tumor cells (about 20%) expressed Ang-1 mRNA in hAng-1-transfected tumors suggesting a silencing of the transgene expression *in vivo* in these tumors. However, compared with the low constitutive expression of Ang-1 in control tumors, the overexpression of hAng-1 in transfected tumors is considerable. Ang-2 mRNA is expressed in control tumors, particularly associated with vessels localized at the tumor borders (**arrows**). hAng-2-overexpressing tumors showed a robust up-regulation of Ang-2 mRNA. There was no increase in Ang-2 expression in hAng-1-transfected tumors. Many tumor vessels are marked by Tie-2 expression (**arrows**). A slight up-regulation of Tie-2 mRNA is observed in hAng-2-overexpressing tumors. All tumors showed high expression levels of VEGF mRNA. Almost all tumor cells expressed VEGF mRNA at this tumor stage. hAng-1 or hAng-2 overexpression did not affect the expression patterns of VEGF as assessed by *in situ* hybridization. Sense control for Ang-1, Ang-2, Tie-2, and VEGF. **Bars**, 50  $\mu\text{m}$ .

We next investigated the expression levels of Tie-2 and VEGF mRNA in the parental and transfected tumors. Tie-2 transcripts were detected in all tumors analyzed. A slightly enhanced Tie-2 signal was detected in hAng-2-overexpressing tumors. *In situ* hybridization revealed that VEGF mRNA was expressed at comparable levels in the different tumors (Figure 3).

#### *Differential Effect of hAng-1 and hAng-2 Overexpression in the Tumor Vasculature*

To assess the effect of overexpression of angiopoietins on the morphology of the tumor vasculature, vibratome slices of 60- $\mu\text{m}$  thickness were stained for von Willebrand factor and analyzed by confocal laser microscopy. The obtained imaging stacks were reconstructed in 3-D view. The tumor vasculature of wild-type and vector only tumors was disorganized with tortuous and dilated vessels of uneven diameter. hAng-1-overexpressing tumors dis-

played a highly branched vascular tree, with vessels of more regular diameter. In contrast, the majority of the vessels in hAng-2-transfected tumors displayed an aberrant structure, characterized by aggregates of endothelial cells forming vessels of narrow lumen and few branches (Figure 4).

#### *Effect of hAng-1 and hAng-2 Overexpression on Tumor Vessel Density and Vessel Count and Tumor Morphology*

We quantitatively analyzed the tumor-associated vasculature, visualized with an antibody to CD31. Initial examination of tumor sections at low magnification showed a relatively uniform vascularization. Micrographs were taken in random areas throughout the tumor tissue. Morphometric analysis revealed an increased number of small vessels (vessel size  $<500 \mu\text{m}^2$ ) in hAng-1-overex-

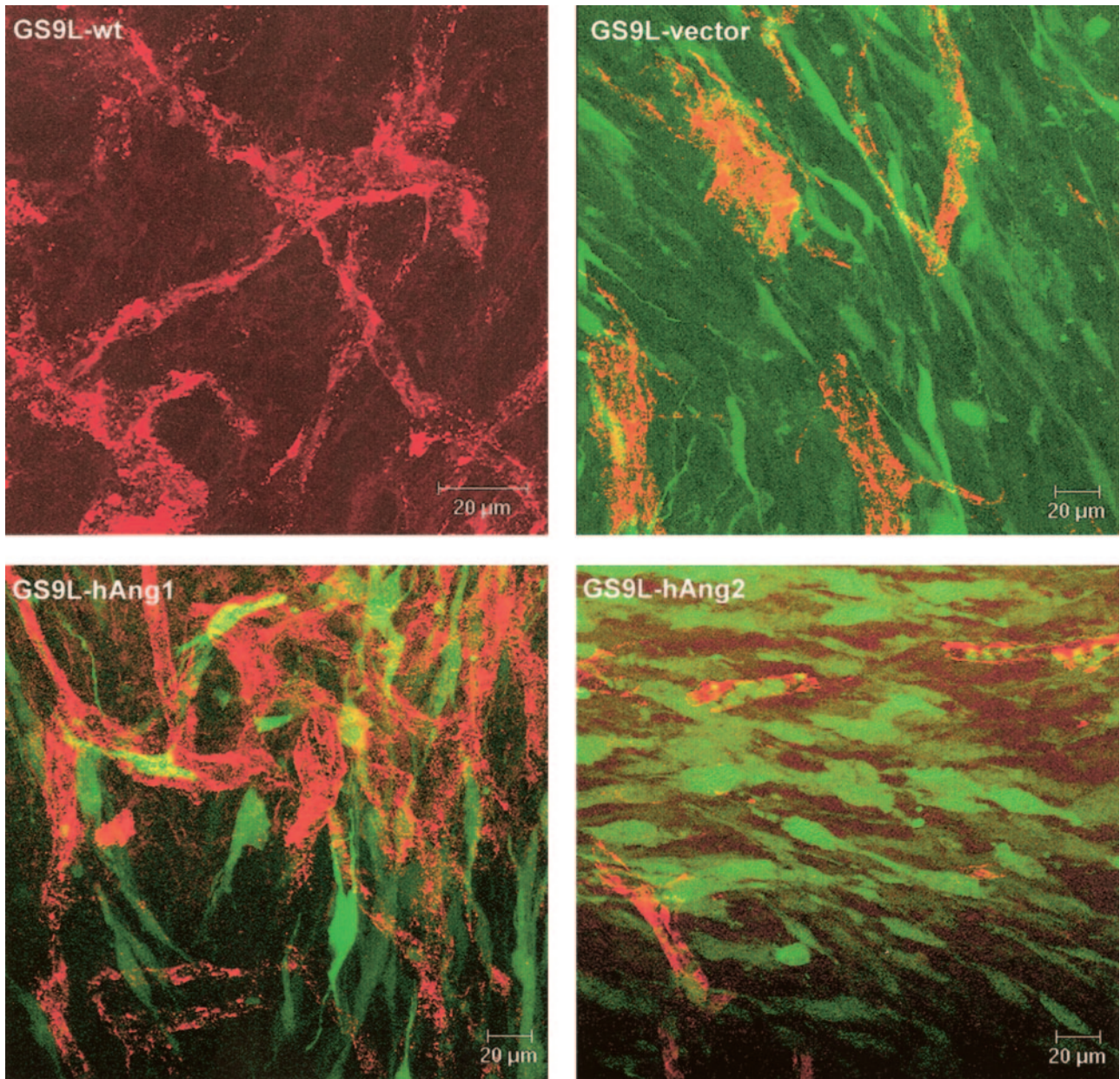


**Figure 4.** Confocal analysis of the vascularization of intracranial tumors 9 days after tumor implantation. Vibratome slices were stained with a rabbit anti-vWF (red). Transfected cells (vector, hAng-1, and hAng-2) expressed the EGFP (green). Tumor derived from parental and vector-transfected cells displayed an irregular vasculature, with vessels of uneven diameter and several shunts. EGFP expression in hAng-1-overexpressing tumors correlates with the finding of *in situ* hybridization, confirming that only a subset of tumor cells expressed the transgene. Nevertheless, hAng-1-overexpressing tumors are highly vascularized with highly branched vessels compared to the control tumors. hAng-2-overexpressing tumors, in contrast, displayed poorly built vessels consisting of small vessels with narrow lumen and few branching. **Bars**, 20  $\mu\text{m}$ .

pressing tumors compared with wild-type and mock-transfected tumors, while no major differences were found in the number of large vessels (vessel size  $>500 \mu\text{m}^2$ ). No major differences were found between control and hAng-2-overexpressing tumors. Comparison of the vessel density in hAng-1-overexpressing tumors with those of control tumors revealed an increase in vessel density. By contrast, decrease in vessel density in hAng-2-overexpressing tumors was observed (Figure 5).

In hAng-2-overexpressing tumors, we observed that glioma cells form tumor cluster around tumor vessels. These tumor masses formed spike-like structures that

invaded the normal brain (Figure 5). When the tumor has grown to form a compact mass, we found tumor cells around the peritumoral vessels but we did not observe tumor cluster that grow beyond the tumor mass.

#### *Overexpression of hAng-1 Results in Increased Vessel Maturation*

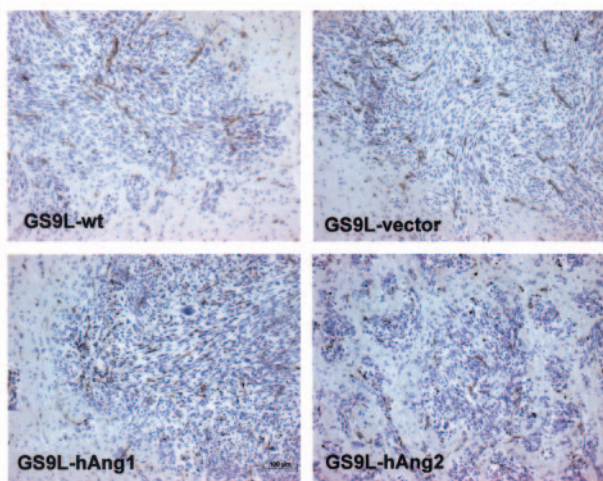
Because the mechanism of angiopoietins might involve the interaction between endothelial and mural cells, we evaluated the pericyte coverage index by immunofluo-

rescence double staining of tumor vessels (vWF, red) and pericytes ( $\alpha$ -SMA, green cells adjacent to endothelial cells). hAng-1 overexpression in GS9L glioma tumors significantly increased the degree of pericyte coverage compared with vector only and wild-type tumors. By contrast, the number of vessels surrounded by pericytes in

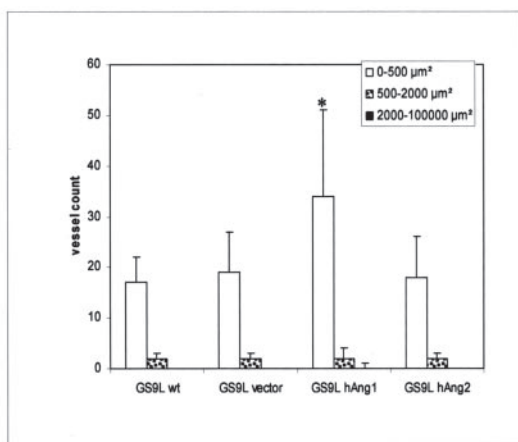
hAng-2-overexpressing tumors was significantly decreased as compared with control tumors (Figure 6).

Transmission electronmicrographs of tumor capillaries from transfected tumors disclosed marked differences in ultrastructural morphology. Pericytes and an intact basement membrane were present in tumors derived from vector only and hAng-1-overexpressing tumors. However, in hAng-2-overexpressing tumors, we observed few pericytes and a discontinuous basement membrane, which did not provide complete vessel coverage. The aberrant morphology of the basement membrane in hAng-2 tumors is characterized by variable thickness and regions with redundant layers. The intercellular junctions were intact. In the tumor center, some vessels showed a complete regression of the endothelial cell layer with only a cavity filled up with cell detritus (Figure 7).

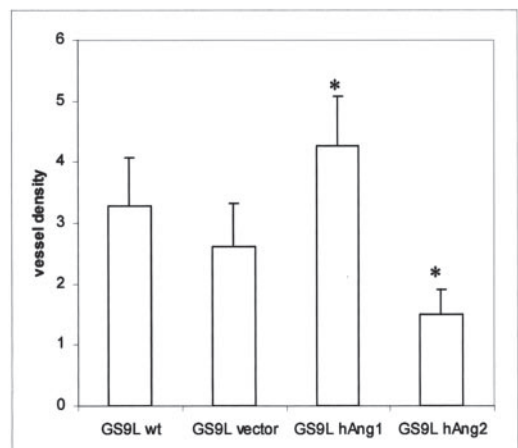
## A



## B



## C



### Assessment of Cell Apoptosis in Tumors

We used the TUNEL method to evaluate whether the reduced tumor growth of the hAng-2 tumors is associated with an increase in apoptosis of tumor cells. TUNEL staining revealed no major differences between the transfected tumors and the control tumors. Several clusters of tumor cells within the tumor and at the tumor border were positively labeled (Figure 8). For technical reasons, double staining using an endothelial cell marker and TUNEL staining to detect specifically endothelial cell death could not be performed.

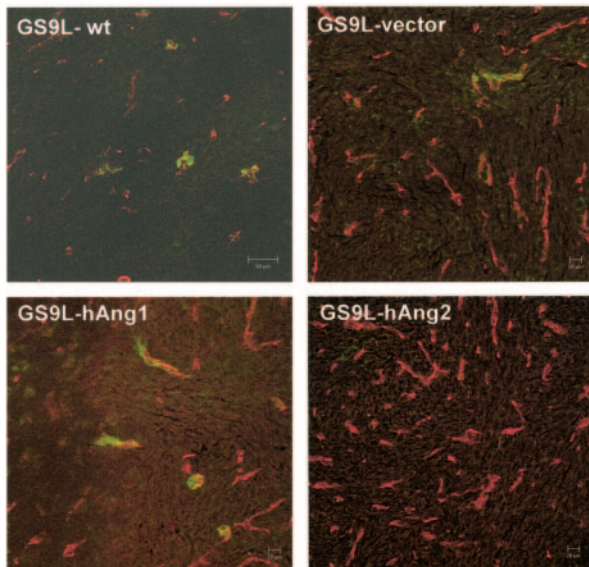
### Effect of Ang-1 and Ang-2 in Capillary Permeability

To study the effect of angiopoietin overexpression on the tumor permeability, the extravasation of Evans blue in tumors was investigated 9 days after tumor implantation. The vascular permeability was measured as an accumulation of Evans blue dye in tumor-bearing hemisphere after circulation for 60 minutes. The absolute Evans blue value was 45 ng/mg brain (SD = 20.6) in control rats (GS9L-wt) while the Evans blue value obtained from rats receiving GS9L-hAng-1 was 60.9 (SD = 35.9) and 16.06 (SD = 11.29) in GS9L-hAng-2. Given the difference in tumor sizes, the calculated Evans blue extravasation values were normalized with the tumor volumes obtained by

**Figure 5.** Morphometric analysis of tumor vasculature. Four animals per group were implanted with parental and transfected tumor cells and sacrificed at day 9 post-implantation. Tumor sections (at least three sections per animal) were stained for CD31. **A:** CD31 immunohistochemistry shows a homogenous distribution of tumor vessels throughout the tumor tissue. **B:** For assessment of tumor vessel count, random fields (three fields/section) were examined at a  $\times 10$  magnification. Blood vessels were counted using Soft Imaging Analysis System and classified according to vessel area (0 to 500  $\mu\text{m}^2$ , 500 to 2000  $\mu\text{m}^2$ , and  $>2000 \mu\text{m}^2$ ). Computer-assisted morphometric analysis of CD31-stained vessels disclosed an increase in number of small vessels (area  $<20 \mu\text{m}^2$ ) in hAng-1-overexpressing tumors. **C:** For assessment of vessel density CD31-stained tumor vessels were evaluated in random fields (five fields per section at a  $\times 20$  magnification) using Soft Imaging Analysis System. Analysis of vessel density revealed an increased vessel density in tumors derived from hAng-1 clone compared to the control tumors, whereas a decrease in vessel density was observed in hAng-2-overexpressing tumors. Data are expressed as mean values and SD (\*,  $P < 0.05$  relative to the wild-type control tumors). **Bar**, 100  $\mu\text{m}$ .



**A**



**B**

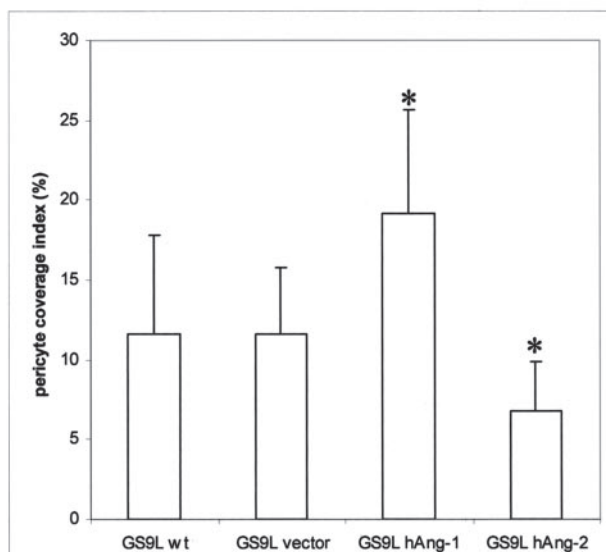


**Figure 6.** Effect of angiopoietin overexpression on pericyte coverage of tumor vessels. **A:** Double-immunofluorescence stains for vWF (red) and  $\alpha$ -SMA (green). Representative fields of wild-type and transfected tumors show increase coverage of tumor vessels in tumors derived from hAng-1-overexpressing cells, while the majority of vessels derived from hAng-2-transfected cells displayed a paucity of SMA-positive periendothelial cells. **B:** Quantitative analysis of the degree of periendothelial cell-associated vessel. The pericyte coverage index is determined by the percentage of tumor vessels that are surrounded by at least one positive SMA-positive periendothelial cell in random fields of the tumor. Data expressed the mean values and SD of at least six fields of tumors obtained from four animals/group. (\*,  $P < 0.05$  relative to the wild-type control tumors). Bars, 50  $\mu$ m and 20  $\mu$ m.

the MRI. Vascular permeability/tumor volume ratio was slightly decreased in hAng-1-overexpressing tumors (mean, 0.63/SD = 0.28) compared to control wild-type tumors (mean, 0.92/SD = 0.22). This difference was not statistically significant. Vascular permeability/tumor vol-

ume ratio was significantly reduced to 0.42 (SD = 0.28) in hAng-2-overexpressing tumors ( $P = 0.016$ ) (Figure 9).

### Discussion

Angiopoietins have been implicated to play a major role in embryonic angiogenesis; however, their exact role in tumor angiogenesis remains still uncertain. This study provides evidence that overexpression of Ang-1 by glioma tumor cells promotes vessel stabilization. Strengthening of the tumor vascular tree may thus explain the increase in glioma growth that we observed in hAng-1-overexpressing tumors. Conversely, the imbalance in the angiopoietin/Tie-2 system created by overexpression of hAng-2 results in disruption of tumor angiogenesis and consequently gave rise to a negative impact on growth of experimental gliomas.

The enhanced tumor angiogenesis in hAng-1-overexpressing tumors found in this study coupled with the strong impairment of sprouting angiogenesis in hAng-2-overexpressing tumors, supports the antagonistic function concept of angiopoietins. In hAng-1-transfected tumors the number of small vessels was significantly increased compared with those in control tumors. Although there was no remarkable difference in vessel count in hAng-2-overexpressing tumors, the vascular density (the area covered by vessels in tumor tissue) was significantly decreased. Gliomas derived from hAng-2-overexpressing cells showed aberrant vessel morphology. Tumor capillaries consisted of small vascular cords with narrow lumen and few sproutings. These findings further corroborate the hypothesis that Ang-2 overexpression disrupts sprouting angiogenesis. The vasculature of hAng-1-overexpressing tumors was more regular with a more constant diameter and several branchings. Collectively, these data support the pro-angiogenic role of Ang-1 in gliomas, whereas the overexpression of its natural antagonist Ang-2 by tumor cells has inhibitory effects on tumor angiogenesis.

Controversial roles for the angiopoietins in tumor angiogenesis and tumor growth have been reported. In breast and colon cancer cells, overexpression of Ang-1 was described to inhibit angiogenesis and tumor growth.<sup>9,11,23,24</sup> In squamous cell carcinoma xenografts, stable overexpression of Ang-1 leads to more than 70% tumor inhibition.<sup>10</sup> On the other hand, overexpression of Ang-1 in human cervical cancer xenografts promotes tumor angiogenesis and inhibits tumor cell apoptosis.<sup>25</sup>

Yu and Stamenkovic<sup>12</sup> found that the overexpression of Ang-2 in Lewis lung carcinoma and TA3 mammary carcinoma cells inhibited the ability to form metastatic tumors and prolonged the survival from tumor-bearing mice. Another study describes a role of Ang-2 in gastric tumor progression.<sup>14</sup> Accordingly, ectopic expression of Ang-2 in hepatocellular carcinoma cells promoted rapid development of human hepatomas within tumors in nude mice.<sup>26</sup> Whether the discrepancy regarding the role of angiopoietins in tumors is dependent on different constitutive expression patterns in a given tissue remains to be elucidated.

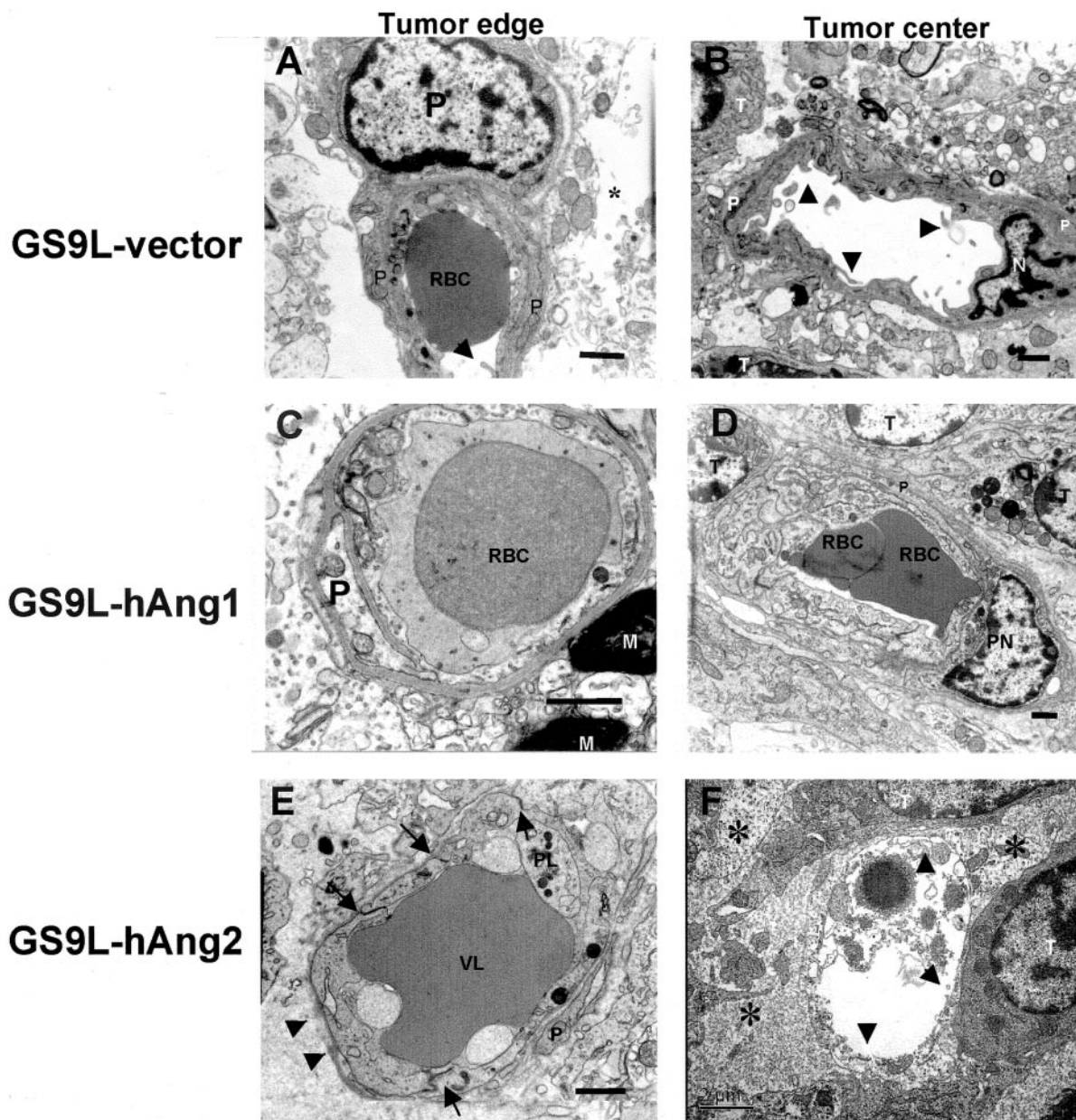


**Figure 7.** Electron micrographs of tumor capillaries in control and tumors overexpressing hAng-1 and hAng-2. Tumor samples were collected at the tumor border and inside the tumor. **A** and **B**: Capillaries of vector-transfected tumors are surrounded by pericytes. The perivascular space is enlarged (\*). Some luminal microfolds enlarged the endothelial surface. Endothelial cell nucleus (N); intraluminal red blood cell (RBC); tumor cell (T). The basement membrane is uniformly thick, compact, and closely opposed to the endothelial cells. **C** and **D**: hAng-1-overexpressing tumors showed capillaries covered by pericytes also in tumor center. The basal membrane in capillaries inside the tumor is surrounded by a structurally abnormal blurred basement membrane but it still provides complete vessel coverage. Myelin in tumor border (M); pericyte nucleus (PN). **E** and **F**: In hAng-2-overexpressing tumors, capillaries at the tumor border were surrounded by a discontinuous basement membrane (arrowheads). Vascular lumen (VL) is filled with fibrin and cell detritus. Pericytes (P) foot has lost the contact with the basement membrane. Intercellular junctions were present (arrows). Endothelial cells were swollen. Complete regression of the endothelial cell layer in a capillary in the center of hAng-2-overexpressing tumor (arrowheads). Bars, 1  $\mu\text{m}$  and 2  $\mu\text{m}$ .

Loss and gain of function experiments showed that the angiopoietin/Tie-2 system is involved in vessel maturation.<sup>4,5,27</sup> Different mechanisms are proposed to explain how the activation of Tie-2 by Ang-1 promotes vascular maturation. A number of clinical and experimental works support the concept that association between the vascular tube and the mural cells mediates vessel stabilization and maturation. It is now widely accepted that Ang-1 binding to Tie-2 recruits periendothelial support cells promoting vessel integrity, whereas Ang-2 induces vessel

destabilization by inducing pericyte drop-off.<sup>28</sup> We demonstrate here that overexpression of hAng-1 increased the percentage of vessels covered by SMA-positive cells. Confocal 3-D analysis of the microvessel architecture from hAng-1 tumors displayed an increase in vascular branching. Localization of pericytes to vessel branching points suggests a role of pericytes in vascular branching morphogenesis.<sup>29</sup> Indeed, pericytes located on sprouts may help guide the growth of endothelial sprouts and contribute to the synthesis of basement membrane on

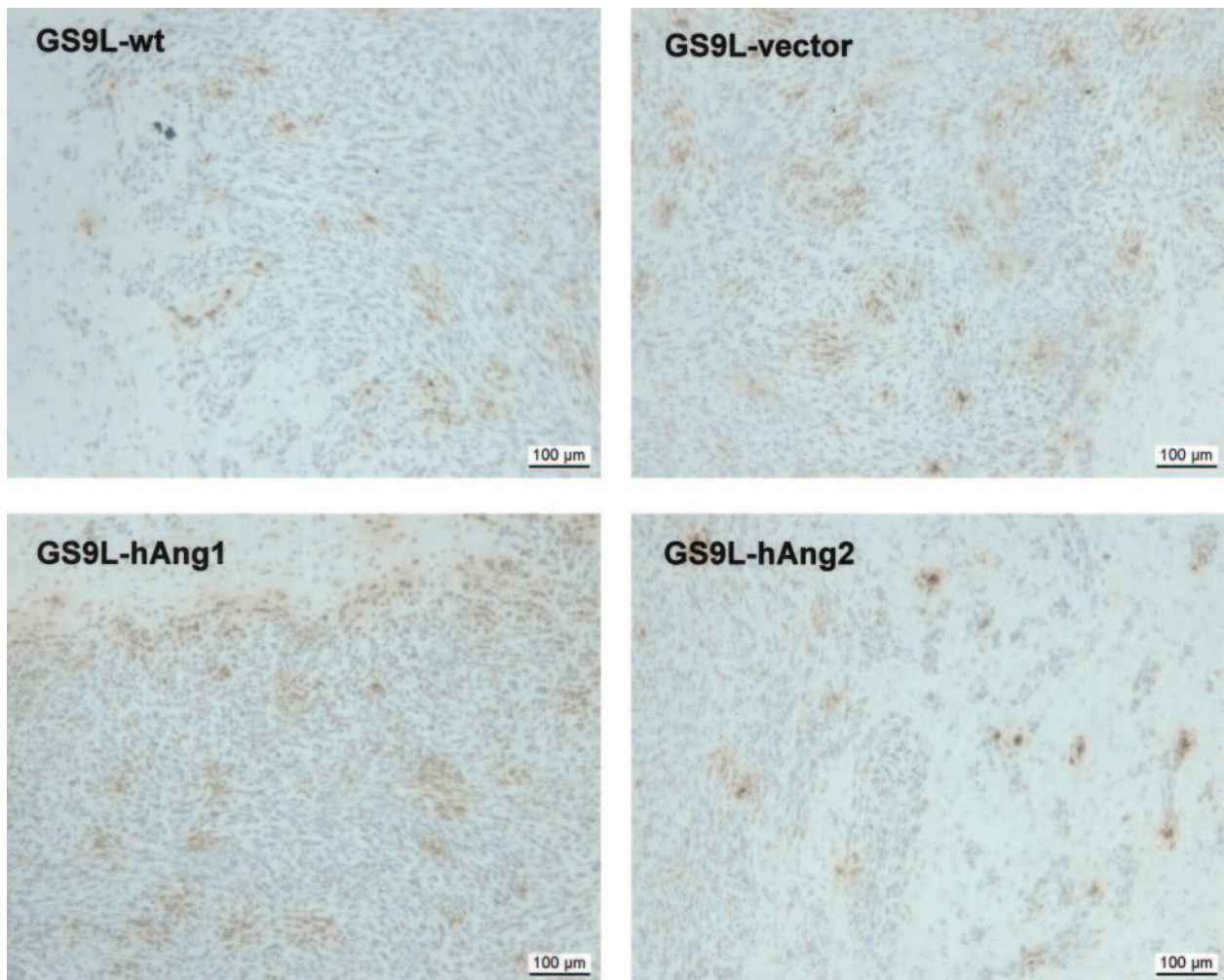


**Figure 8.** hAng-2 overexpression did not increase tumor cell apoptosis. For detection of apoptotic cells, TUNEL assay was performed. TUNEL staining revealed no major differences between the transfected tumors and the control tumors. Several clusters of tumor cells within the tumor were positively labeled. **Bars,** 100  $\mu\text{m}$ .

blood vessel. Thus, it is plausible to speculate that the increased levels of Ang-1 in gliomas may contribute to increased pericyte recruitment resulting in capillary sprouting and maintenance of tumor vessel maturation and integrity. As a consequence of the increased number of mature tumor vessels, a more functional vascular network can stimulate tumor growth.

It is believed that angiogenesis may start with the degradation of the vascular basement membrane and drop-off of pericytes.<sup>28</sup> Ang-2 promotes loss of endothelial cell interaction with support cells and the extracellular matrix.<sup>30</sup> This process requires the cooperation of Ang-2 with VEGF, which supply the endothelial cells with the critical survival signals that are otherwise provided by cell-cell and cell-ECM contact.<sup>31</sup> We show here that hAng-2 overexpression by tumor cells significantly decreased the number of vessels covered with pericytes. These results corroborate the concept that an increased expression of Ang-2 might prevent pericyte coverage inhibiting endothelial sprouting and in later stages leads to vessel regression. In models of tumor and retina neovascularization, Benjamin et al<sup>32</sup> found that pericytes promote endothelial survival and prevent vessel regression

after VEGF withdrawal. The aberrant morphology of vessels in Ang-2-overexpressing tumors suggested that increased levels of Ang-2 impair capillary sprouting and induce vessel regression. We detected high amounts of VEGF mRNA in all tumors including hAng-2-overexpressing tumors. Thus, we speculate that even high amounts of VEGF cannot prevent the signaling cascade triggered by high levels of Ang-2 that result in vessel regression.

Angiopoietins might also exert their effects on the vessel maturation and stabilization through mechanisms independent of pericyte recruitment. Recent observations have shown that Tie-2 phosphorylation induced by Ang-1 may promote survival signals in endothelial cells by activating the phosphatidylinositol 3' inositol kinase Akt transduction pathway.<sup>33</sup> Ang-1 might also interact directly with extracellular matrix compounds and mediate the stabilizing effects through integrins.<sup>34</sup> Ang-1 can also induce the localization of platelet endothelial cell adhesion molecule (PECAM) into junctions between endothelial cells strengthening these junctions. Accordingly, it has been shown that also high concentrations of Ang-2 can be an apoptosis survival factor for endothelial cells through the activation of the Tie-2 receptor, PI 3'-kinase, and Akt.<sup>35</sup> *In*

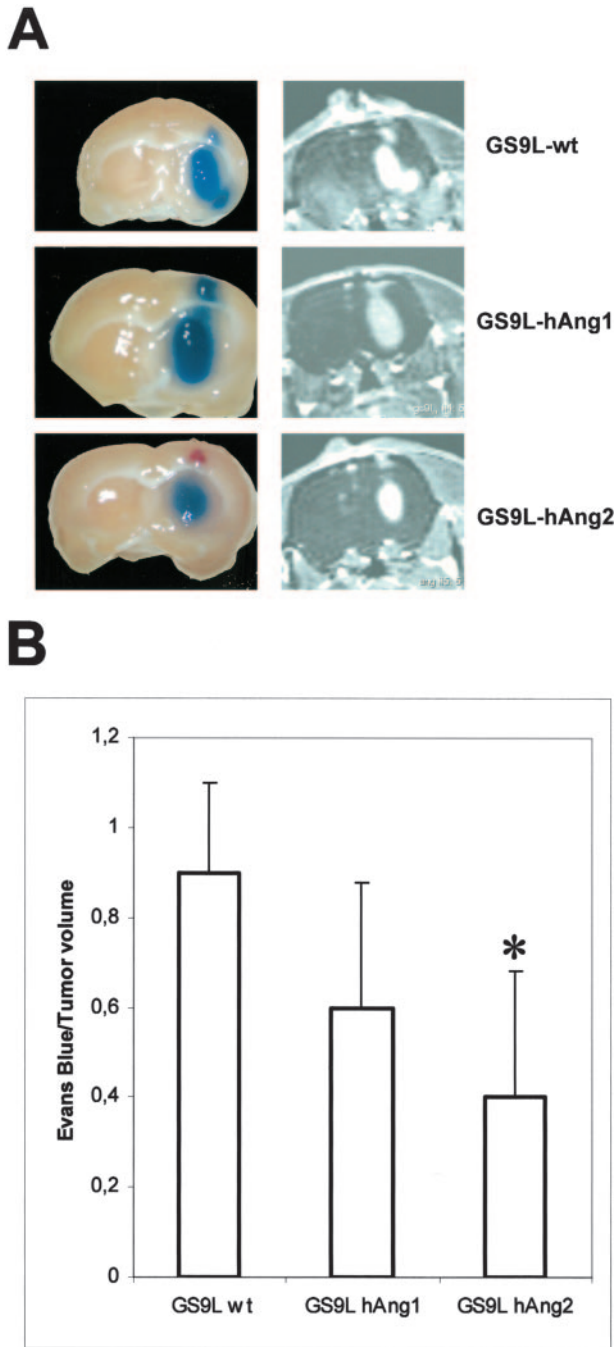


**Figure 9.** Capillary permeability in GS9L-wt-, GS9L-hAng-1-, and GS9L-hAng-2-derived tumors. **A:** Rats were injected intravenously with a 2% Evans blue solution and, after 60 minutes, were then perfused with PBS. Brains were then removed and photographed. MRI scans of corresponding slices obtained immediately before the Evans blue injection. **B:** Quantitative analysis of Evans blue extravasation from brain extracts. Data are expressed as ratio of amount of extravasated Evans blue (ng/gram of brain) per tumor volume ( $\text{mm}^3$ ). Evans blue was spectrophotometrically quantified at 620 nm. As control for perfusion efficiency, the absorbance of the contralateral hemisphere was subtracted from that of the hemisphere ipsilateral to the tumor. For each group  $n = 5$ .  $P < 0.05$  relative to wild-type control tumors.

*in vivo*, it has been shown that in the presence of endogenous VEGF, Ang-2 stimulates sprouting of new blood vessels. By contrast, Ang-2 promotes endothelial cell death and vessel regression if the activity of endogenous VEGF is inhibited.<sup>36</sup> TUNEL assay disclosed clusters of

apoptotic cells throughout the tumor tissue. We did not observe an increase in apoptosis associated with the reduced growth of hAng-2 tumors. For technical reasons, we could not investigate the apoptotic endothelial cells using TUNEL assay. However, transmission EM analysis of hAng-2-overexpressing tumors disclosed several tumor vessels surrounded by an abnormal basement membrane, with regions where the basement membrane appeared discontinuous beside regions where it appeared multi-layered. In some vessels, we observed a complete regression of endothelial cells leaving strands of basement membrane devoid of their endothelial cell coverage. Taken together, in this glioma model hAng-2 overexpression induces vessel regression even in the presence of high levels of VEGF. Thus, a tight quantitative and spatial balance between VEGF, Ang-1, and Ang-2 seems to be a key in the regulation of capillary sprouting and regression.

Ang-2 has been shown to activate metalloproteases like MMP-2 and thereby inducing tumor invasion in an experimental glioma model.<sup>37</sup> In hAng-2-overexpressing tumors, we observed that clusters of tumor cells containing a central vessel core were interspersed in the normal brain tissue. In other areas tumors formed a compact mass and displayed at the tumor borders spike-like tumor clusters invading the peritumor brain along a peritumor vessel. However, we did not observe cluster of tumor cells located far away from the main tumor mass. We hypothesize that impairment of angiogenesis resulting from hAng-2 overexpression favors vessel co-option, which rendered tumors a morphological aspect of a more invasive phenotype.

Ang-1 can prevent vessel permeability in different settings. Transgenic overexpression of Ang-1 in skin under the control of the keratin promoter turned the vessel more leakage resistant.<sup>27</sup> When Ang-1 was systemically delivered using an adenoviral approach, vessels became less leaky in response to topical and inflammatory stimuli or local injection of VEGF.<sup>38</sup> Although Ang-1 is known to induce resistance to vascular leakage in skin vessels this might not be the case for tumor vessels. Using the vascular extravasation of Evans blue dye we tested whether the overexpression of angiopoietins affect the vascular permeability in gliomas. The brain tissue content of Evans blue was increased in rats bearing tumors transfected with hAng-1 compared to control tumors whereas the Evans blue leakage in the ipsilateral hemisphere of hAng-2-transfected tumors was reduced. Considering that the hAng-1 tumors displayed an increased volume, the increase in the amount of Evans blue extravasation in the tumor tissue might simply reflect vascular density of tissue and not the permeability of individual tumor capillaries. To minimize the effect of tumor volume in the amount of Evans blue we calculated the ratio of Evans blue amounts and the tumor volume obtained in magnetic resonance tomography (MRT). By doing so we found that the vascular permeability/tumor volume ratio in hAng-1-derived tumors is lower than in control tumors. However, this data should be analyzed with caution since evaluation of Evans blue leakage is a static measurement of a dynamic process. Several factors like tumor size, capillary density, tumor perfusion, and blood flow can affect

the overall Evans blue leakage observed in brain tissue. The reduced capillary density might be responsible for the reduction in Evans blue/tumor size obtained in the hAng-2-overexpressing tumors. Certainly dynamic measures like evaluation of capillary permeability coefficient *in vivo* by means of dynamic contrast-enhanced MRT will provide insightful data to clarify this issue.

In glioblastoma tissues and experimental gliomas *in situ* hybridization revealed Ang2 mRNA in endothelial cells but not in glioma cells.<sup>19</sup> Expression profiling of Ang-2 indicates that it acts primarily as an autocrine regulator of endothelial cell function. In our experiments, we evaluated the paracrine Ang-2 overexpression in a tumor model. Whether paracrine and autocrine Ang-2 expression will differentially modulate angiogenesis is currently unknown. According to our results, paracrine Ang-2 functions as a negative regulator of tumor angiogenesis.

Blocking the function of Tie-2 signaling is a potential means to test the effect of the Tie-2/angiopoietin system in tumor angiogenesis. Furthermore, whether the Ang/Tie-2 pathway represents a good target for anti-angiogenic therapies remains a debatable issue. Stratman et al<sup>39</sup> showed that a dominant-negative Tie-2 construct led to 15% growth inhibition in Tie-2-negative murine mammary tumors as opposed to 57% growth inhibition in Tie-2-positive tumors. Interruption of Tie-2 signaling either via siRNA<sup>8</sup> or overexpression of kinase-dead Tie-2<sup>40</sup> lead to a loss of endothelial cell viability. Recently, Zadeh et al<sup>41</sup> showed that inhibition of Tie-2 using a kinase-deficient Tie-2 construct decreases growth of malignant human astrocytomas subcutaneous and intracranial xenografts. It has been suggested that the Ang-1-mediated stabilization effect of tumor vessels might be a desirable therapeutic technique to inhibit new vessel formation and therefore arrest tumor growth.<sup>11</sup> Our results in gliomas suggest the opposite: vascular stabilization might be instrumental for promoting and sustaining tumor angiogenesis. Creating an imbalance among the angiopoietins by overexpression of Ang-2 might therefore provide the means to disrupt angiogenesis and control tumor growth.

### Acknowledgments

We thank Prof. J. Zentner (Department of Neurosurgery, University of Freiburg, Freiburg, Germany) and Prof. B. Volk (Department of Neuropathology, University of Freiburg, Freiburg, Germany) for long-lasting support; Mrs. Renate Wirtz for excellent technical assistance in electron microscopic studies; Mrs. Jasmin Korbmacher and Ms. Jadranka Macas for technical assistance; and Dr. Urban Deutsch (MPI, Münster, Germany) for helping with the cloning techniques.

### References

1. Carmeliet P, Jain RK: Angiogenesis in cancer and other diseases. *Nature* 2000, 407:249–257
2. Hanahan D, Folkman J: Patterns and emerging mechanisms of the angiogenic switch during tumorigenesis. *Cell* 1996, 86:353–364

3. Davis S, Aldrich TH, Jones PF, Acheson A, Compton DL, Jain V, Ryan TE, Bruno J, Radziejewski C, Maisonpierre PC, Yancopoulos GD: Isolation of angiopoietin-1, a ligand for the TIE2 receptor, by secretion-trap expression cloning. *Cell* 1996, 87:1161–1169
4. Maisonpierre PC, Suri C, Jones PF, Bartunkova S, Wiegand SJ, Radziejewski C, Compton D, McClain J, Aldrich TH, Papadopoulos N, Daly TJ, Davis S, Sato TN, Yancopoulos GD: Angiopoietin-2, a natural antagonist for Tie2 that disrupts *in vivo* angiogenesis. *Science* 1997, 277:55–60
5. Suri C, Jones PF, Patan S, Bartunkova S, Maisonpierre PC, Davis S, Sato TN, Yancopoulos GD: Requisite role of angiopoietin-1, a ligand for the TIE2 receptor, during embryonic angiogenesis. *Cell* 1996, 87:1171–1180
6. Witzenbichler B, Maisonpierre PC, Jones P, Yancopoulos GD, Isner JM: Chemotactic properties of angiopoietin-1 and -2, ligands for the endothelial-specific receptor tyrosine kinase Tie2. *J Biol Chem* 1998, 273:18514–18521
7. Iurlaro M, Scatena M, Zhu WH, Fogel E, Wieting SL, Nicosia RF: Rat aorta-derived mural precursor cells express the Tie2 receptor and respond directly to stimulation by angiopoietins. *J Cell Sci* 2003, 116:3635–3643
8. Shim WS, Teh M, Mack PO, Ge R: Inhibition of angiopoietin-1 expression in tumor cells by an antisense RNA approach inhibited xenograft tumor growth in immunodeficient mice. *Int J Cancer* 2001, 94:6–15
9. Hayes AJ, Huang WQ, Yu J, Maisonpierre PC, Liu A, Kern FG, Lippman ME, McLeskey SW, Li LY: Expression and function of angiopoietin-1 in breast cancer. *Br J Cancer* 2000, 83:1154–1160
10. Hawighorst T, Skobe M, Streit M, Hong YK, Velasco P, Brown LF, Riccardi L, Lange-Asschenfeldt B, Detmar M: Activation of the tie2 receptor by angiopoietin-1 enhances tumor vessel maturation and impairs squamous cell carcinoma growth. *Am J Pathol* 2002, 160:1381–1392
11. Tian S, Hayes AJ, Metheny-Barlow LJ, Li LY: Stabilization of breast cancer xenograft tumour neovasculature by angiopoietin-1. *Br J Cancer* 2002, 86:645–651
12. Yu Q, Stamenkovic I: Angiopoietin-2 is implicated in the regulation of tumor angiogenesis. *Am J Pathol* 2001, 158:563–570
13. Ahmad SA, Liu W, Jung YD, Fan F, Reinmuth N, Bucana CD, Ellis LM: Differential expression of angiopoietin-1 and angiopoietin-2 in colon carcinoma: a possible mechanism for the initiation of angiogenesis. *Cancer* 2001, 92:1138–1143
14. Etoh T, Inoue H, Tanaka S, Barnard GF, Kitano S, Mori M: Angiopoietin-2 is related to tumor angiogenesis in gastric carcinoma: possible *in vivo* regulation via induction of proteases. *Cancer Res* 2001, 61:2145–2153
15. Tanaka S, Sugimachi K, Yamashita Y, Shirabe K, Shimada M, Wands JR, Sugimachi K: Angiogenic switch as a molecular target of malignant tumors. *J Gastroenterol* 2003, 38(Suppl 15):93–97
16. Plate KH, Breier G, Risau W: Molecular mechanisms of developmental and tumor angiogenesis. *Brain Pathol* 1994, 4:207–218
17. Stratmann A, Risau W, Plate KH: Cell type-specific expression of angiopoietin-1 and angiopoietin-2 suggests a role in glioblastoma angiogenesis. *Am J Pathol* 1998, 153:1459–1466
18. Zagzag D, Hooper A, Friedlander DR, Chan W, Holash J, Wiegand SJ, Yancopoulos GD, Grumet M: *In situ* expression of angiopoietins in astrocytomas identifies angiopoietin-2 as an early marker of tumor angiogenesis. *Exp Neurol* 1999, 159:391–400
19. Koga K, Todaka T, Morioka M, Hamada J, Kai Y, Yano S, Okamura A, Takakura N, Suda T, Ushio Y: Expression of angiopoietin-2 in human glioma cells and its role for angiogenesis. *Cancer Res* 2001, 61:6248–6254
20. Machein MR, Risau W, Plate KH: Antiangiogenic gene therapy in a rat glioma model using a dominant-negative vascular endothelial growth factor receptor 2. *Hum Gene Ther* 1999, 10:1117–1128
21. Uyama O, Okamura N, Yanase M, Narita M, Kawabata K, Sugita M: Quantitative evaluation of vascular permeability in the gerbil brain after transient ischemia using Evans blue fluorescence. *J Cereb Blood Flow Metab* 1988, 8:282–284
22. Eberhard A, Kahlert S, Goede V, Hemmerlein B, Plate KH, Augustin HG: Heterogeneity of angiogenesis and blood vessel maturation in human tumors: implications for antiangiogenic tumor therapies. *Cancer Res* 2000, 60:1388–1393
23. Stoeltzing O, Ahmad SA, Liu W, McCarty MF, Parikh AA, Fan F, Reinmuth N, Bucana CD, Ellis LM: Angiopoietin-1 inhibits tumour

- growth and ascites formation in a murine model of peritoneal carcinomatosis. *Br J Cancer* 2002, 87:1182–1187
24. Stoeltzing O, Ahmad SA, Liu W, McCarty MF, Wey JS, Parikh AA, Fan F, Reinmuth N, Kawaguchi M, Bucana CD, Ellis LM: Angiopoietin-1 inhibits vascular permeability, angiogenesis, and growth of hepatic colon cancer tumors. *Cancer Res* 2003, 63:3370–3377
  25. Shim WS, Teh M, Bapna A, Kim I, Koh GY, Mack PO, Ge R: Angiopoietin 1 promotes tumor angiogenesis and tumor vessel plasticity of human cervical cancer in mice. *Exp Cell Res* 2002, 279:299–309
  26. Tanaka S, Mori M, Sakamoto Y, Makuuchi M, Sugimachi K, Wands JR: Biologic significance of angiopoietin-2 expression in human hepatocellular carcinoma. *J Clin Invest* 1999, 103:341–345
  27. Thurston G, Suri C, Smith K, McClain J, Sato TN, Yancopoulos GD, McDonald DM: Leakage-resistant blood vessels in mice transgenically overexpressing angiopoietin-1. *Science* 1999, 286:2511–2514
  28. Pettersson A, Nagy JA, Brown LF, Sundberg C, Morgan E, Jungles S, Carter R, Krieger JE, Manseau EJ, Harvey VS, Eckelhoefer IA, Feng D, Dvorak AM, Mulligan RC, Dvorak HF: Heterogeneity of the angiogenic response induced in different normal adult tissues by vascular permeability factor/vascular endothelial growth factor. *Lab Invest* 2000, 80:99–115
  29. Nehls V, Schuchardt E, Drenckhahn D: The effect of fibroblasts, vascular smooth muscle cells, and pericytes on sprout formation of endothelial cells in a fibrin gel angiogenesis system. *Microvasc Res* 1994, 48:349–363
  30. Lauren J, Gunji Y, Alitalo K: Is angiopoietin-2 necessary for the initiation of tumor angiogenesis? *Am J Pathol* 1998, 153:1333–1339
  31. Holash J, Wiegand SJ, Yancopoulos GD: New model of tumor angiogenesis: dynamic balance between vessel regression and growth mediated by angiopoietins and VEGF. *Oncogene* 1999, 18:5356–5362
  32. Benjamin LE, Hemo I, Keshet E: A plasticity window for blood vessel remodelling is defined by pericyte coverage of the pre-formed endothelial network and is regulated by PDGF-B and VEGF. *Development* 1998, 125:1591–1598
  33. Niu Q, Perruzzi C, Voskas D, Lawler J, Dumont DJ, Benjamin LE: Inhibition of Tie-2 signaling induces endothelial cell apoptosis, decreases Akt signaling, and induces endothelial cell expression of the endogenous anti-angiogenic molecule, thrombospondin-1. *Cancer Biol Ther* 2004, 3:402–405
  34. Carlson TR, Feng Y, Maisonpierre PC, Mrksich M, Morla AO: Direct cell adhesion to the angiopoietins mediated by integrins. *J Biol Chem* 2001, 276:26516–26525
  35. Kim I, Kim JH, Moon SO, Kwak HJ, Kim NG, Koh GY: Angiopoietin-2 at high concentration can enhance endothelial cell survival through the phosphatidylinositol 3'-kinase/Akt signal transduction pathway. *Oncogene* 2000, 19:4549–4552
  36. Lobov IB, Brooks PC, Lang RA: Angiopoietin-2 displays VEGF-dependent modulation of capillary structure and endothelial cell survival in vivo. *Proc Natl Acad Sci USA* 2002, 99:11205–11210
  37. Hu B, Guo P, Fang Q, Tao HQ, Wang D, Nagane M, Huang HJ, Gunji Y, Nishikawa R, Alitalo K, Cavenee WK, Cheng SY: Angiopoietin-2 induces human glioma invasion through the activation of matrix metalloproteinase-2. *Proc Natl Acad Sci USA* 2003, 100:8904–8909
  38. Thurston G, Rudge JS, Ioffe E, Zhou H, Ross L, Croll SD, Glazer N, Holash J, McDonald DM, Yancopoulos GD: Angiopoietin-1 protects the adult vasculature against plasma leakage. *Nat Med* 2000, 6:460–463
  39. Stratmann A, Acker T, Burger AM, Amann K, Risau W, Plate KH: Differential inhibition of tumor angiogenesis by tie2 and vascular endothelial growth factor receptor-2 dominant-negative receptor mutants. *Int J Cancer* 2001, 91:273–282
  40. Lin P, Buxton JA, Acheson A, Radziejewski C, Maisonpierre PC, Yancopoulos GD, Channon KM, Hale LP, Dewhirst MW, George SE, Peters KG: Antiangiogenic gene therapy targeting the endothelium-specific receptor tyrosine kinase Tie2. *Proc Natl Acad Sci USA* 1998, 95:8829–8834
  41. Zadeh G, Qian B, Okhowat A, Sabha N, Kontos CD, Guha A: Targeting the Tie2/Tek receptor in astrocytomas. *Am J Pathol* 2004, 164:467–476